JHR 98: 1–18 (2025)
doi: 10.3897/jhr.98.136200
https://jhr.pensoft.net

RESEARCH ARTICLE

JOURNAL OF Hymenoptera RESEARCH
A peer-reviewed open-access journal
The International Society of Hymenopterists

New wasps of †Falsiformicidae from mid-Cretaceous Kachin amber

Zhen Wang[1], Alexandr P. Rasnitsyn[2], Evgeny E. Perkovsky[3], Lars Vilhelmsen[3], Taiping Gao[1]

1 *College of Life Sciences, Capital Normal University, Beijing, 100048, China* **2** *A. A. Borissiak Palaeontological Institute, Russian Academy of Sciences, Moscow, 117647, Russia* **3** *Natural History Museum of Denmark, SCIENCE, University of Copenhagen, Copenhagen, 2100, Denmark*

Corresponding authors: Taiping Gao (tpgao@cnu.edu.cn); Alexandr P. Rasnitsyn (alex.rasnitsyn@gmail.com)

Academic editor: Brendon Boudinot | Received 3 September 2024 | Accepted 3 December 2024 | Published 3 January 2025

https://zoobank.org/77736D1C-30F9-4D6C-8310-3A04121CACE2

Citation: Wang Z, Rasnitsyn AP, Perkovsky EE, Vilhelmsen L, Gao T (2025) New wasps of †Falsiformicidae from mid-Cretaceous Kachin amber. Journal of Hymenoptera Research 98: 1–18. https://doi.org/10.3897/jhr.98.136200

Abstract

Two new species of the family †Falsiformicidae Rasnitsyn, 1975, *Siccibythus robustus* **sp. nov.** and *Siccibythus aristovi* **sp. nov.**, are described from the mid-Cretaceous Kachin amber based on three well-preserved specimens. The new species belongs to †*Siccibythus* Cockx & McKellar, 2016, based on the elongate pronotum and fore wing with cells 2+3rm and 3r not enclosed with tubular veins. We summarize the diversity and distribution for all species of †Falsiformicidae and provide a revised key to the family. These new findings enhance the diversity of †Falsiformicidae in Kachin amber.

Keywords

Cenomanian, Kachin amber, key to genera and species, morphological characters, new species

Introduction

In recent years, a large number of insect species have been discovered in Kachin amber (Zhang et al. 2018; Ross 2024). During the mid-Cretaceous, for more than 20 Ma (Heine et al. 2004; Seton et al. 2012) the West Myanmar Terrane was geographically isolated as an island in the Tethys Ocean between Asia and the Indian tectonic block, far from both of them (Westerweel et al. 2019; Yang et al. 2023) or, alternatively, was already a part of Laurasia (Sevastjanova et al. 2016). It has been suggested that the organisms found in Kachin

Copyright *Zhen Wang et al.* This is an open access article distributed under the terms of the Creative Commons Attribution License (CC BY 4.0), which permits unrestricted use, distribution, and reproduction in any medium, provided the original author and source are credited.

amber evolved from a selection of tropical or subtropical life forms that once inhabited the supercontinent of Gondwana (Poinar 2018). Without doubt, Kachin amber is the most diverse single deposit in the mid-Cretaceous (Ross 2024; Wang et al. 2024; Wu et al. 2024).

†Falsiformicidae Rasnitsyn, 1975 is a small extinct family characterized by a 12-segmented antenna in female, a 13-segmented antenna in male; the hind wing without closed cells; and a node-like first metasomal tergum. The family and its first species, †*Falsiformica cretacea* Rasnitsyn, 1975, were described in upper Cenomanian amber from Nizhnyaya Agapa in the Taimyr from incomplete male and female specimens, considered to be of the same species (Rasnitsyn 1975) which he placed in Scolioidea. For many years there were no additional records of this family until Perrichot et al. (2014) reported the discovery of some undescribed species in Cretaceous ambers from France, Lebanon, Myanmar and Spain. Lucena and Melo (2018) mentioned that †*Burmomyrma* Dlussky, 1996 (Dlussky 1996) is likely to belong to †Falsiformicidae, confirming this awaits re-examination of the holotype. Regardless, *Burmomyrma* cannot be attributed to any known genus of †Falsiformicidae because it is described as lacking closed cells in the forewing.

Rasnitsyn et al. (2020) transferred two recently described species of Scolebythidae, †*Cursoribythus silvestris* Cockx and McKellar, 2016 and †*Siccibythus musculosus* Cockx and McKellar, 2016, to †Falsiformicidae, making them the second and third genera of the family. However, Lepeco and Melo (2024) transferred †*Cursoribythus* to Bethylidae based on head shape, scape somewhat slender, bidentate claws, and long pronotum (hiding the propleura in dorsal view). Rasnitsyn et al. (2020) suggested that †Falsiformicidae belongs to Vespoidea and described five new species of †*Siccibythus*: *S. oculatus*, *S. pallidus*, *S. martynovae*, *S. ohmkuhnlei* and *S. paulus*. Engel (2022) published the first species of †Falsiformicidae found in New Jersey amber, †*Neophenax orcus* Engel, 2022. Engel (2022) presents several important ideas about the phylogenetic position and classification of †Falsiformicidae, suggesting that it is more closely related to Chrysidoidea. We discuss this in more detail below (see Discussion). Recently, Zhang et al. (2024) described a new genus and species, †*Falsiformix pedestris* Zhang & Rasnitsyn, 2024, discovered in Kachin amber. All species of †Falsiformicidae are listed in Table 1.

Table 1. Diversity and distribution of †Falsiformicidae.

Species	Locality	Horizon	References
Falsiformica cretacea	Nizhnyaya Agapa, Taimyr Peninsula, N. Siberia	?upper Cenomanian	Rasnitsyn 1975
Falsiformix pedestris	Myanmar, Hukawng Valley	lowermost Cenomanian	Zhang et al. 2024
Neophenax orcus	USA, New Jersey	Turonian amber	Engel 2022
Siccibythus aristovi sp. nov.	Myanmar, Hukawng Valley	lowermost Cenomanian	Present study
Siccibythus martynovae	Myanmar, Hukawng Valley	lowermost Cenomanian	Rasnitsyn et al. 2020
Siccibythus musculosus	Myanmar, Hukawng Valley	lowermost Cenomanian	Cockx and McKellar 2016
Siccibythus oculatus	Myanmar, Hukawng Valley	lowermost Cenomanian	Rasnitsyn et al. 2020
Siccibythus ohmkuhnlei	Myanmar, Hukawng Valley	lowermost Cenomanian	Rasnitsyn et al. 2020
Siccibythus pallidus	Myanmar, Hukawng Valley	lowermost Cenomanian	Rasnitsyn et al. 2020
Siccibythus paulus	Myanmar, Hukawng Valley	lowermost Cenomanian	Rasnitsyn et al. 2020
Siccibythus robustus sp. nov.	Myanmar, Hukawng Valley	lowermost Cenomanian	Present study

Herein, we describe two new species, †*Siccibythus robustus* sp. nov. and †*Siccibythus aristovi* sp. nov., from mid-Cretaceous Kachin amber. We provide some diversity statistics, as well as a revised key to the genera and species in †Falsiformicidae. These new discoveries enrich the diversity of the family found in Kachin amber.

Material and methods

The Kachin amber specimens CNU-HYM-MA-2016212, CNU-HYM-MA-2016213 and CNU-HYM-MA-2016214, were purchased by Mr. Fangyuan Xia on September 1, 2014, and donated to the Key Laboratory of Insect Evolution and Environmental Changes, College of Life Sciences, Capital Normal University, Beijing, China, in September 2014. The fossils were all collected in full compliance with the laws of Myanmar and China. All specimens are permanently deposited in well-established, public museums (Key Laboratory of Insect Evolution and Environmental Changes, College of Life Sciences, Capital Normal University, Beijing, China), in full compliance with the International Code of Zoological Nomenclature and the Statement of the International Palaeoentomological Society (International Commission on Zoological Nomenclature 1999; Szwedo et al. 2020).

The amber specimens were examined under a Leica M205C dissecting microscope. Photographs were taken with a Nikon SMZ 25 microscope with an attached Nikon DS-Ri2 digital camera system. The wing venation terminology follows that of Goulet and Huber (1993), with additional morphological terminology following that of Rasnitsyn et al. (2020).

The measurements follow Schödl (2007) and Boudinot and Fisher (2013), with some additions and a few modifications to the acronyms (indicated by an asterisk *). Definitions of length, width, and height are based on Goulet and Huber (1993). Measurements were recorded in millimeters to two decimal places using the Nikon DS-Ri2 digital camera system mounted on Nikon SMZ 25 microscope. The measurement data are listed in Suppl. material 1. The measurement error is less than 10% of the measured data. The error calculation is based on most measurements of specimen CNU-HYM-MA2016212 conducted independently by three researchers, each performing three measurements. The standard deviation is derived from the resulting nine data points. Detailed data and standard deviation analysis are presented in Suppl. material 2.

Measurements

Total body length *. Maximum length from the anterior head capsule to the distal end of the last metasomal segment.

Head length *. Maximum between two vertical parallel lines in the lateral view of the head: one at the anterior margin near the eyes and the other at the posterior margin of the occiput.

Head width. Maximum width of head capsule behind the eyes, in full-face view.

Head height. Maximum length of head capsule, excluding mandibles, measured from anterior margin of clypeus to nuchal carina, with both in same plane of focus.

Scape length. Maximum length of the scape excluding basal constriction.

Pedicel length *. Maximum length of the pedicel.

The first flagellum length *. Maximum length of the the first flagellum.

Total flagellum length *. Combined length of all flagellar segments.

Wing length *. Maximum length of the wing base to margin.

Leg segments length *. Maximum length from the apex to the base of each segment of legs.

The first metasomal segment length *. Maximum length of the first metasomal tergum measured with anterior and posterior margins in same plane of focus.

Metasoma length *. Maximum length from the base of the first metasomal segment to the last metasomal apex, excluding the genitalia in males and the sting in females.

Systematic palaeontology

Order Hymenoptera Linnaeus, 1758

Family †Falsiformicidae Rasnitsyn, 1975

Type genus. †*Falsiformica* Rasnitsyn, 1975.

Genera included. †*Falsiformica* Rasnitsyn, 1975, †*Siccibythus* Cockx & McKellar, 2016, †*Neophenax* Engel, 2022, *Falsiformix* Zhang & Rasnitsyn, 2024.

Genus *Siccibythus* Cockx & McKellar, 2016

Type species. *Siccibythus musculosus* Cockx & McKellar, 2016.

Species included. *Siccibythus musculosus* Cockx & McKellar, 2016, *S. martynovae* Rasnitsyn, Zhang, Müller& Zhang, 2020, *S. oculatus* Rasnitsyn, Zhang, Müller & Zhang, 2020, *S. ohmkuhnlei* Rasnitsyn, Zhang, Müller & Zhang, 2020, *S. pallidus* Rasnitsyn, Zhang, Müller & Zhang, 2020, *S. paulus* Rasnitsyn, Zhang, Müller & Zhang, 2020, *S. aristovi* sp. nov. and *S. robustus* sp. nov.

Revised diagnosis. Propodeum weakly sculptured with longitudinal carinae; antenna with 13 segments in male, 12 in female, scape elongate and flattened, pedicel weakly pyriform; three or four labial palpomeres; fore wing with no cells closed with tubular veins in its middle and distal part, vein 1m-cu at most only partially tubular; vein R1 absent apical to pterostigma, and apical parts of M, M+Cu and A (distally of Cu-a) spectral. Fore tarsus and mid tarsus with large, bilobed arolium, smaller arolium present on hind tarsus, claws simple.

Remarks. †*Siccibythus* Cockx & McKellar, 2016 differs †*Falsiformica* Rasnitsyn, 1975 and †*Neophenax* Engel, 2022 by having fore wing with vein 1m-cu at most partially tubular and pronotum with dorsal surface longer than wide or, rarely, subquadrate. †*Siccibythus* Cockx & McKellar, 2016 differs from †*Falsiformix* Zhang & Rasnitsyn, 2024 in having a fore wing longer than mesosoma.

***Siccibythus robustus* Wang, Rasnitsyn, Perkovsky & Vilhelmsen, sp. nov.**
https://zoobank.org/6F39958F-FB10-4AB2-9752-9AAB01FECDE8

Diagnosis. The length of the scape is less than 0.3 times the length of the flagellum. Fore wing with 2Rs distal of r-rs several times as long as r-rs; Cu nebulous. Fore tibial spur long, thin and acute apically. Metabasitarsus longer than tarsomeres 2–4 combined. Propodeum outline angular. Anterior outline of 1st metasomal tergum somewhat angular.

Etymology. The species is named after the Latin adjective *robustus*, meaning "thick" and referring to the thick fore femur.

Type material. ***Holotype*** • female. No. CNU-HYM-MA2016212. A well-preserved and complete specimen (Figs 1, 2). ***Paratype*** • male. No. CNU-HYM-MA2016213. A well-preserved and complete specimen (Figs 3, 4).

Type locality and horizon. The amber specimens were collected from Kachin, northern Myanmar, lowermost Cenomanian, mid-Cretaceous, which was dated at 98.79 ± 0.62 Ma (Cruickshank and Ko 2003; Shi et al. 2012).

Description. Female. Head globose, with eyes bulging, occupying most of lateral parts of head (except for wide, convex temples), almost reaching mandibular bases, occipital carina complete, reaching hypostomal carina well behind mandibular base, vertex and frons narrow, longer than wide, ocelli in small acute triangle well distant from eyes, interantennal space flat, clypeus short, simple. Antenna slender, with 12 antennomeres in female (13 in male), each antennomere is approximately 1–2 times longer than wide, scape slightly longer than pedicel and first flagellomere combined, pedicel longer than first flagellomere, flagellomeres slightly shortening gradually toward apex except for shorter first flagellomere and longer apical segment (Fig. 1B). Labrum not visible externally, mandibles small, overlapping, maxillary and labial palps not visible (paratype can be observed mandibles with three teeth, maxillary palp with four palpomeres visible, three apical long, narrow).

Pronotum posterior margin extended, with pronotum accounting for 0.4 times the length of mesosoma, pronotum short declivitous part delimited by transverse groove posteriorly. Propleura long, slender, abutting throughout ventrally. Mesoscutum convex between notauli; notauli complete, parapsides and lateral edges incomplete; notauli widely spaced anteriorly, converging to almost meet posteriorly; transscutal articulation distinct; mesoscutellum triangular, narrow, the length is 0.4 times its maximum width, weakly convex, carinate laterally. Meso- and metapleuron smooth, metapleuron delimited from propodeum with incomplete row of pits (Fig. 2A, B). Metanotum short, with indistinct metascutellum in female (metanotum short, with distinct metascutellum in male). Propodeum with clear dorsal and posterior surfaces meeting in angle, dorsal with longitudinal and one transverse carinae, posterior surface with lateral longitudinal carinae, sublateral longitudinal carinae and supracoxal transverse carinae (Fig. 2B).

Fore wing distal of basal veins (1Rs and 1M), r-rs and 1cu-a without tubular veins, except for pterostigma and half section of 2Rs distal of r-rs, all other distal veins nebulous in female (fore wing distal of basal vein (1Rs and 1M) and cu-a with no tubular veins, except for pterostigma, r-rs and most of Rs distal of r-rs, all other veins nebulous in male). Pterostigma prominent, longer than wide; vein 1Rs straight, shorter than

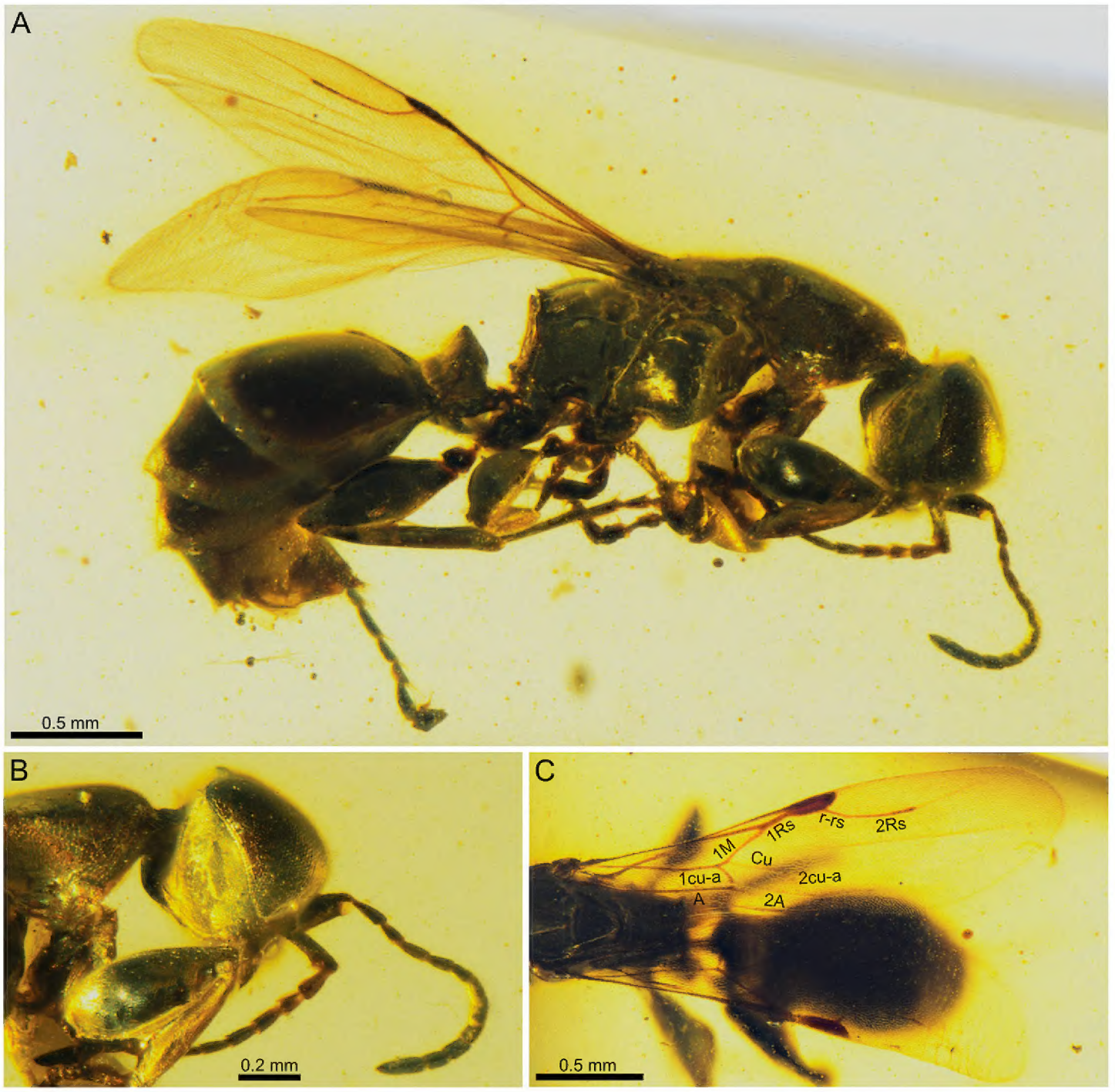

Figure 1. Photographs of *Siccibythus robustus* sp. nov. (Female holotype; CNU-HYM-MA-2016212) **A** habitus in lateral view **B** head in lateral view **C** fore wing venation.

1M, arise from Sc+R just proximal to pterostigma; 1cu-a shorter than 1M, placed distinctly before it, parallel to 2cu-a; Cu parallel to A; vein A extending distal to 1cu-a, and distal part tubular, extending distal to 2cu-a as nebulous vein, both 1cu-a and 2cu-a reaching A; r-rs slightly curved, arising beyond midlength of pterostigma; r-m not present (Fig. 1C). Hind wing with thin, tubular veins Rs arising from Sc+R; A present; other veins not visible. Seven hamuli present.

Fore coxa swollen, triangular, nearly as long as wide; fore trochanter short, fore trochantellus not visible in female (fore trochantellus trapezoidal, the ratio compared to the length of the fore femur is approximately 1:17 in male); fore femur swollen in middle, twice as long as wide (calcar long, thin, gently curved and acute apically in male); fore tibia nearly as long as femur; fore tarsus shorter than fore tibia, basitarsomere shorter than combined length of remaining tarsomeres in female (basitarsomere longer than com-

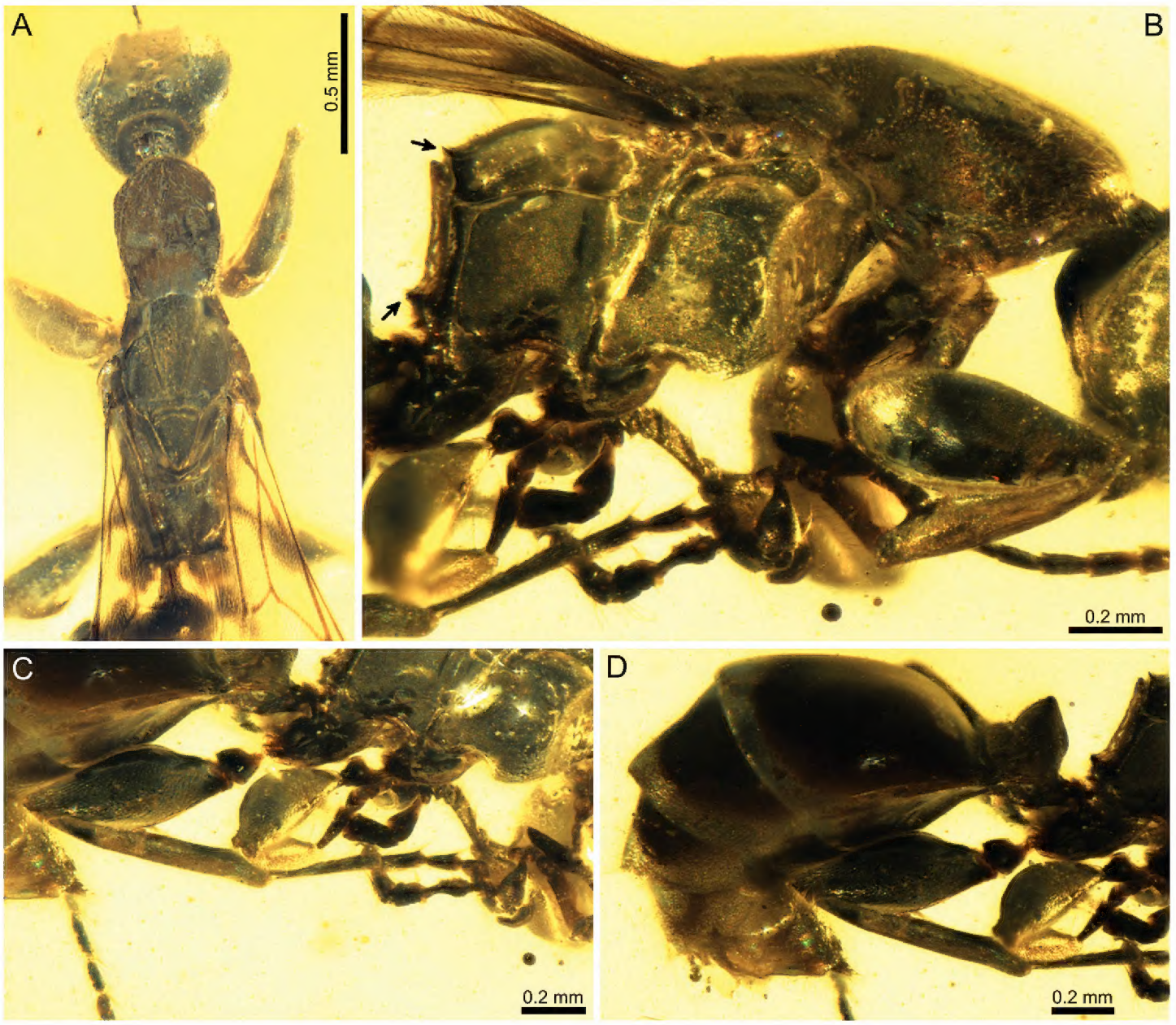

Figure 2. Photographs of *Siccibythus robustus* sp. nov. (Female holotype; CNU-HYM-MA-2016212) **A** mesosoma in dorsal view **B** mesosoma in lateral view, arrowheads indicate metapleural-propodeal boundary, black arrow indicates the carinae **C** hind leg in lateral view **D** metasoma in lateral view.

bined length of remaining tarsomeres in male). Mid coxa slender, smaller than both fore and hind coxa, twice as long as wide; mid trochanter short, mid trochantellus very short and ring-like, approximately 0.1 times as long as femur; mid femur swollen in middle, twice as long as wide; mid tibia slenderer than femur, three times as long as wide, tibia shorter than femur; mid tarsus nearly as long as mid tibia, basitarsomere shorter than combined length of remaining tarsomeres. Hind coxae elongate, swollen, three times as long as wide, with lamella dorsally, basally in female (no lamella in male); hind trochanter short, bulging dorsally, hind trochantellus very short and ring-like (ca. 0.02 as long as femur); hind femur swollen in middle, nearly three times as long as wide in female (nearly six times as long as wide in male); hind tibia very slender, slightly longer than femur; hind tarsus nearly as long as hind tibia, basitarsomere slightly shorter than combined length of remaining tarsomeres (Fig. 2C). Claw simple, arolium small. Tibial spur formula 1/2/2.

First metasomal segment short, tergum node-like, female with anterior outline, low triangular, second metasomal segment longest and highest, following segments

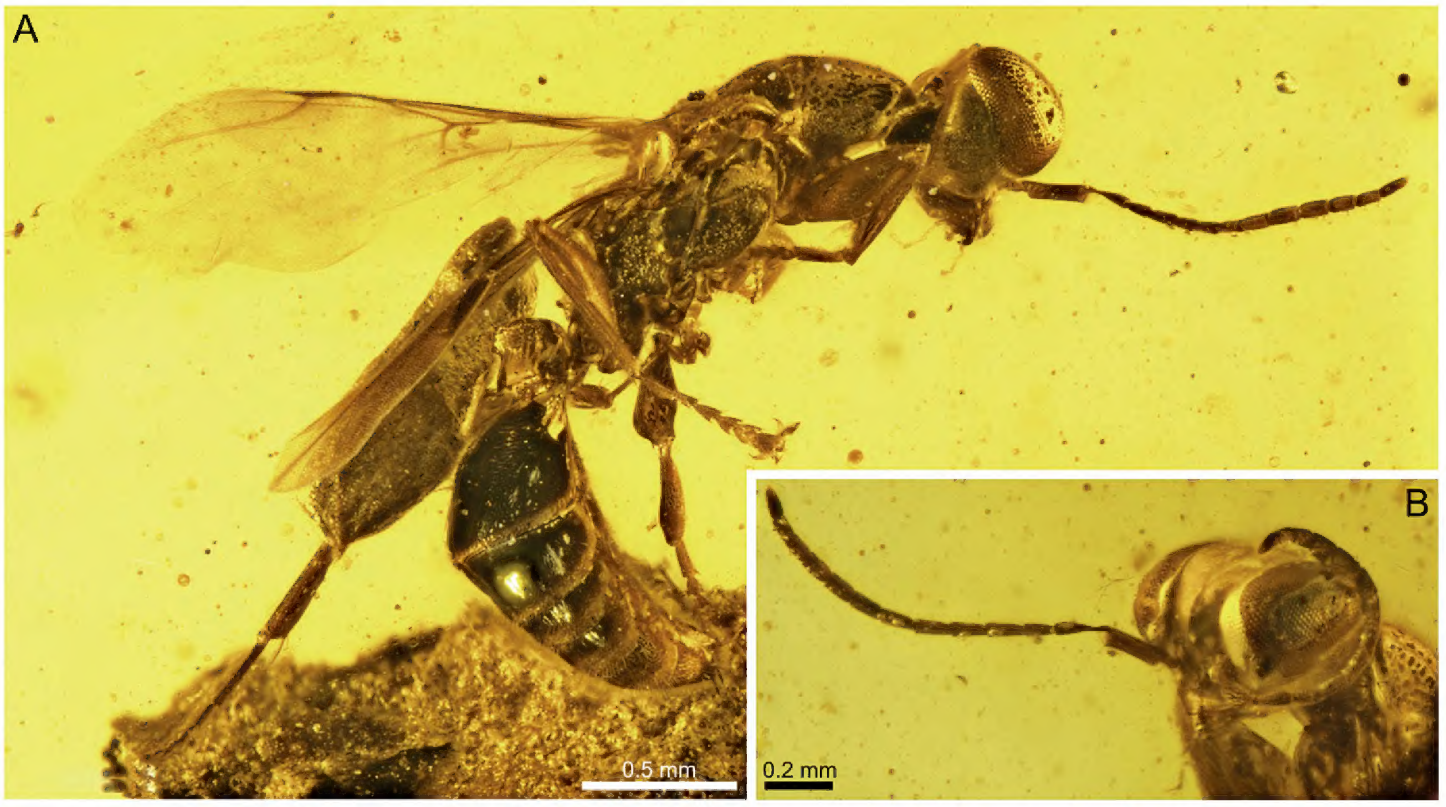

Figure 3. Photographs of *Siccibythus robustus* sp. nov. (Male paratype; CNU-HYM-MA-2016213) **A** habitus in lateral view **B** head in lateral view.

gradually smaller, apical metasomal sternum high, with dorsal sides overlapping (Fig. 2D) (male first metasomal tergum with fore surface convex, dorsal surface short, rather flat, elevated above hind surface; seventh metasomal sternum with two long upcurved teeth).

Measurements (mm). Holotype female. Total body length (excluding sting and antenna) 3.93; head length 0.47, width 0.61, height 0.53; scape length 0.25, pedicel length 0.13, the first flagellum length 0.08, total flagellum length 0.87; fore wing length 2.22; hind wing length 1.56; fore coxa length 0.30, fore trochanter length 0.57, fore femur length 0.58, fore tibia length 0.55, fore tarsal length 0.32; mid coxa length 0.31, mid trochanter length 0.09, mid trochantellus 0.05, mid femur length 0.50, mid tibia length 0.38, mid tarsal length 0.38; hind coxa length 0.44, hind trochanter length 0.14, hind trochantellus 0.02, hind femur length 0.67, hind tibia length 0.78, hind tarsal length 1.02; the first metasomal segment length 0.28, metasoma length 2.18.

Paratype male. Total body length (excluding antenna) 3.54; head length 0.50, width 0.42, height 0.50; scape length 0.25, pedicel length 0.16, the first flagellum length 0.09; total flagellum length 0.99; fore wing length 1.98; hind wing length 1.47; fore coxa length 0.21, fore trochanter length 0.08, fore trochantellus 0.03, fore femur length 0.50, fore tibia length 0.45, fore tarsal length 0.32; mid coxa length 0.12, mid trochanter length 0.10, fore trochantellus 0.02, mid femur length 0.40, mid tibia length 0.30, mid tarsal length 0.34; hind coxa length 0.28, hind trochanter length 0.12, hind femur length 0.55, hind tibia length 0.60, hind tarsal length 0.57; the first metasomal segment length 0.25, metasoma length 1.62.

Remarks. The new species is classified in †*Siccibythus* Cockx & McKellar, 2016 based on the fore wing with no cells closed with tubular veins in its middle and distal

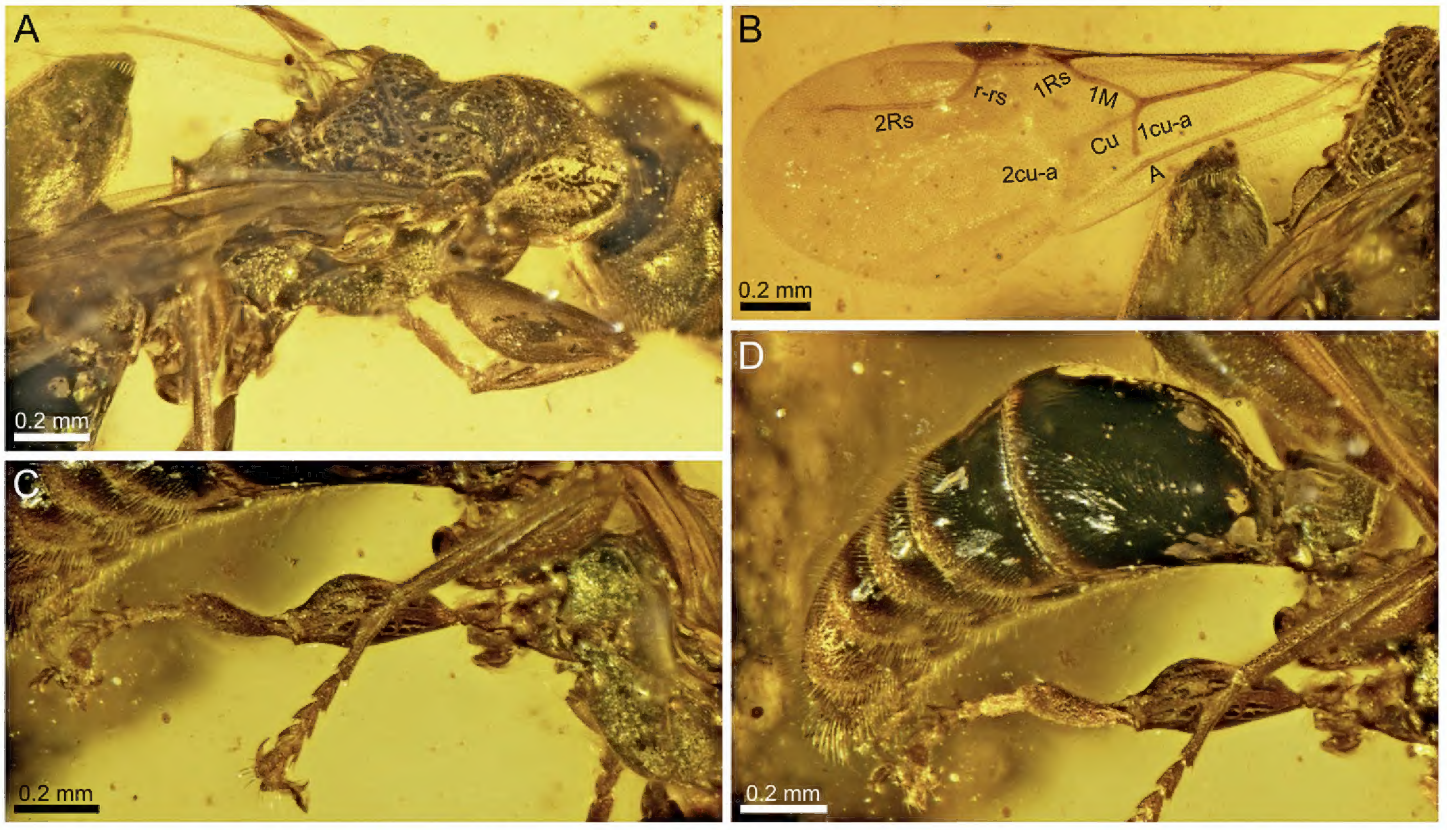

Figure 4. Photographs of *Siccibythus robustus* sp. nov. (Male paratype; CNU-HYM-MA-2016213) **A** mesosoma in dorsal view **B** fore wing venation **C** hind leg in lateral view **D** metasoma in lateral view.

part (Rasnitsyn et al. 2020). However, the new species is differentiated from *Siccibythus martynovae*, *S. pallidus* and *S. oculatus* by fore wing with 2Rs distal of r-rs several times as long as r-rs, basitarsus longer than tarsomeres 2–4 combined (vs. 2Rs distal of r-rs at most about as long as r-rs, basitarsus not longer than tarsomeres 2–4 combined in *S. martynovae*, *S. pallidus* and *S. oculatus*). It is distinguished from *S. musculosus* by the following characters: 1) Cu is nebulous (vs. Cu is tubular); 2) calcar long, thin and acute apical (vs. calcar short, bifid apically). It is differentiated from *S. paulus* by the length of the scape being less than 0.3 times the length of the flagellum (vs. the scape is longer than or equal to 0.3 times of the flagellum). It is distinguished from *S. ohmkuhnlei* by the following characters: 1) anterior outline of 1st metasomal tergum somewhat angular (vs. straight); 2) propodeum outline angular (vs. more smoothly curved).

***Siccibythus aristovi* Wang, Rasnitsyn, Perkovsky & Vilhelmsen, sp. nov.**
https://zoobank.org/C0027405-25CC-48BB-AD21-8FCA112E21F0

Diagnosis. Fore wing with 2Rs distal of r-rs at most about as long as r-rs; Rs+M and Cu both nebulous; A behind 1cu-a not pigmented (except for very base). Fore tibial spur short, bifid apically. Basitarsus not longer than tarsomeres 2–4 combined. Pronotum short, propodeal horns long.

Etymology. The specific name "*aristovi*" is dedicated to the memory of the late Dr. Daniil Sergeevich Aristov, for his outstanding contribution to palaeoentomology.

Type material. ***Holotype*** • female. No. CNU-HYM-MA2016214. A well-preserved and complete specimen (Figs 5, 6).

Type locality and horizon. The amber specimen was collected from Kachin, northern Myanmar, lowermost Cenomanian, mid-Cretaceous, which was dated at 98.79 ± 0.62 Ma (Cruickshank and Ko 2003; Shi et al. 2012).

Description. Female. Body brown, metasoma dark brown. Head globose, with eyes bulging, occupying three-quarters of head in lateral view, almost reaching mandibular bases, occipital carina complete, reaching hypostomal carina well behind mandibular base, ocelli in small acute triangle well distant from eyes, interantennal space flat. Antenna narrow, with 12 antennomeres, each antennomere is approximately 1–2 times longer than wide, scape shorter than pedicel, pedicel longer than first flagellomere, flagellomeres slightly shortening gradually toward apex except for longer apical segment (Fig. 6A). Mandibles with three teeth, not overlapping; labrum not visible; maxillary palp short with six elongate palpomeres, labial palp short, with four slightly elongate to subquadrate palpomeres (Fig. 6B).

Pronotum with long dorsal part shorter than wide before lateral lobes, constricted near midlength, with fore declivitous part short, delimited by transverse groove posteriorly. Propleura long, slender, in lateral view, the length is 4 times its width, and abutting throughout. Mesoscutum with deep notauli widely spaced anteriorly, converging to almost meet posteriorly; transscutal articulation distinct; mesoscutellum rather short, wide apically, weakly convex. Meso- and metapleurae smooth. Metanotum short, with metascutellum very short and wide. Propodeum with dorsal and posterior surfaces meeting in angle, dorsal with longitudinal carina, and with transverse one midway between sublateral carinae, posterior surface with lateral longitudinal carinae, sublateral longitudinal carinae and supracoxal transverse carinae (Fig. 6C, D).

Fore wing basal veins (C, Sc+R, M+Cu, A, 1Rs and 1M), r-rs, short pterostigma, part of 2Rs distal of r-rs and cu-a tubular, other veins nebulous. Pterostigma prominent, longer than wide; vein 1Rs straight, shorter than 1M, arise from Sc+R just proximal to pterostigma; 1cu-a shorter than 1M, parallel to 2cu-a, placed slightly basally of 1M; 1Cu parallel to A; vein A extends distal up to 1cu-a only; r-rs straight, arising beyond midlength of pterostigma; r-m not present (Fig. 6E). Hind wing with Sc+R; other veins not visible.

Fore trochanter present, fore trochantellus ring-like; fore femur slightly swollen in middle, nearly three times as long as wide; fore tibia shorter than femur, calcar acute (not bifid); fore tarsus shorter than fore tibia, basitarsomere shorter than combined length of remaining tarsomeres. Mid trochanter present, mid trochantellus ring-like; mid femur slightly swollen in middle, four times as long as wide; mid tibia nearly as long as femur, six times as long as wide; mid tarsus shorter than mid tibia, basitarsomere shorter than combined length remaining tarsomeres. Hind trochanter short, bulging dorsally, hind trochantellus ring-like; hind femur slightly swollen in middle, nearly four times as long as wide; hind tibia slender than femur, longer than femur; hind tarsus nearly as long as hind tibia, remaining tarsomeres combined shorter than basitarsomere. Claw simple, arolium small. Tibial spur formula 1/2/2.

First metasomal segment short, tergum node-like, triangular in lateral view, with anterior surface concave, second segment slightly longer and higher than following, following gradually smaller, apical (sixth) sternum high, apparently folded, with upper sides and apical orifice apparently not specialized, tergum 7 as visible (in lateral view)

Figure 5. Photographs of *Siccibythus aristovi* sp. nov. (Female holotype; CNU-HYM-MA-2016214) **A** habitus in dorsal view **B** habitus in lateral view.

small but more or less sclerotized, with spiracle not enlarged (Fig. 6F). Sting straight, apparently short, without teeth.

Measurements (mm). Holotype female. Total body length (excluding sting and antenna) 4.14; head length 0.94, width 0.62, height 0.48; scape length 0.20, pedicel length 0.19, the first flagellum length 0.14, total flagellum length 1.11; fore wing length 1.95; hind wing length 1.20; fore coxa length 0.27, fore trochantellus 0.06, fore femur length 0.64, fore tibia length 0.49, fore tarsal length 0.64; mid coxa length 0.25, mid trochanter length 0.10, mid trochantellus 0.04, mid femur length 0.60, mid tibia length 0.64, mid tarsal length 0.39; hind coxa length 0.23, hind trochanter length 0.10, hind trochantellus 0.06, hind femur length 0.69, hind tibia length 0.58, hind tarsal length 0.79; the first metasomal segment length 0.29, metasoma length 1.66.

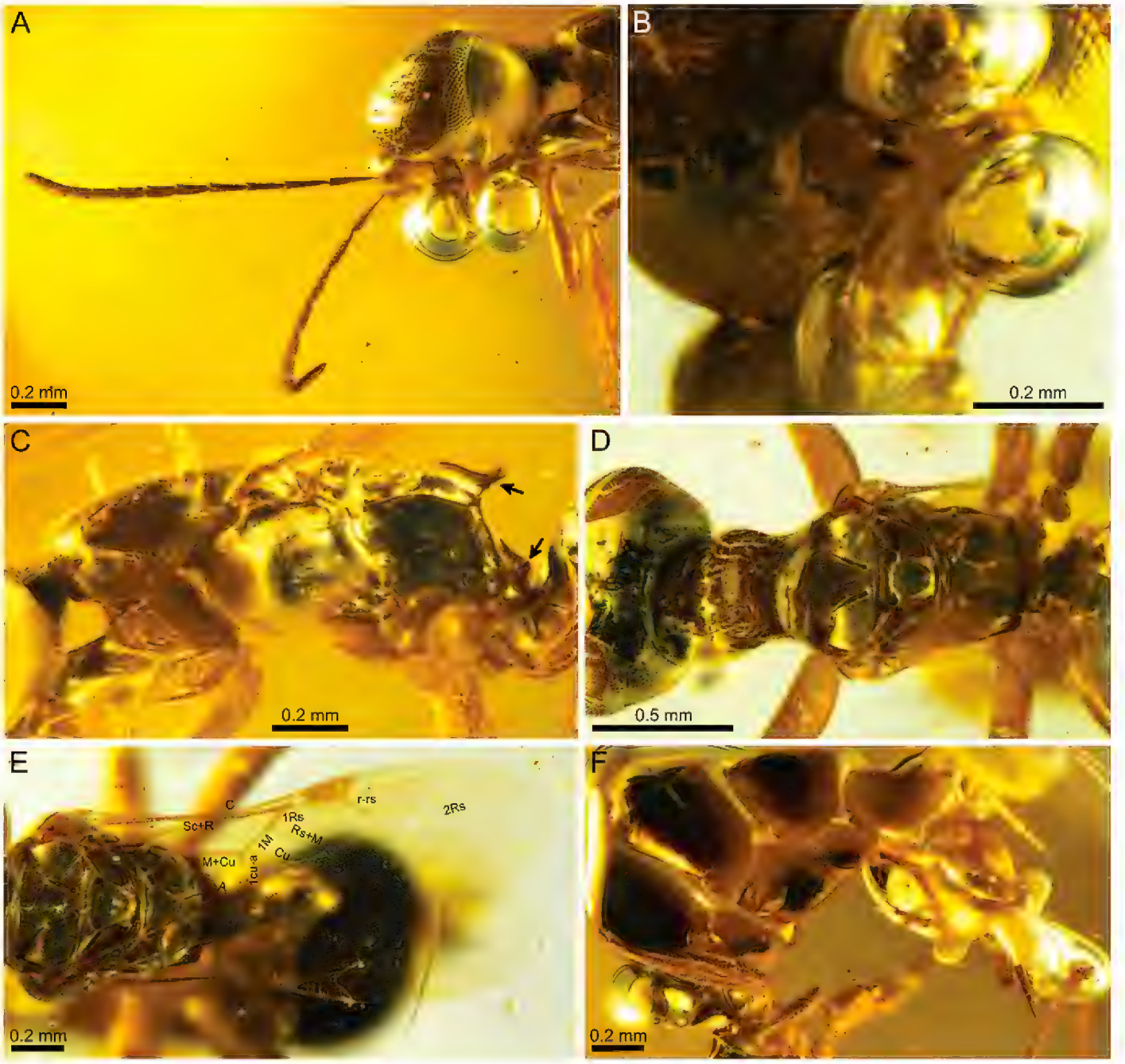

Figure 6. Photographs of *Siccibythus aristovi* sp. nov. (Female holotype; CNU-HYM-MA-2016214) **A** head in lateral view **B** mouthparts **C** mesosoma in lateral view, black arrow indicates the carinae **D** mesosoma in dorsal view **E** fore wing venation **F** metasoma in lateral view.

Remarks. The new species is classified in †*Siccibythus* Cockx & McKellar, 2016 based on the fore wing with no cells closed with tubular veins in its middle and distal part (Rasnitsyn et al. 2020). It is differentiated from *Siccibythus musculosus*, *S. paulus*, *S. ohmkuhnlei* and *S. robustus* by fore wing with 2Rs distal of r-rs shorter than r-rs, basitarsus not longer than tarsomeres 2–4 combined (vs. 2Rs distal of r-rs several times as long as r-rs, basitarsus longer than tarsomeres 2–4 combined in *S. musculosus*, *S. paulus*, *S. ohmkuhnlei* and *S. robustus*). It is distinguished from *S. martynovae* by fore wing veins Rs+M and Cu both being nebulous (vs. Rs+M and Cu are both tubular in *S. martynovae*). It is differentiated from *S. pallidus* by the following characters: 1) fore wing with 2A not pigmented (except for very base) (vs. fore wing with 2A pigmented); 2) pronotum constricted in the middle (vs. not constricted). It is distinguished from *S. oculatus* by pronotum short, propodeal horns long (vs. pronotum long, propodeal horns short).

Key to genera and species of †Falsiformicidae

1 Brachypterous, with forewing about as long as mesosoma ..... ***Falsiformix pedestris* Zhang & Rasnitsyn, 2024**

– Macropterous, having a fore wing longer than mesosoma **2**

2 Fore wing with 1m-cu completely tubular (Engel 2022, fig. 24); pronotum with dorsal surface distinctly wider than long medially **3**

– Fore wing with 1m-cu at most partially tubular; pronotum with dorsal surface longer than wide or, rarely, subquadrate **4**

3 Pedicel shorter than 1st flagellomere; fore wing with 2-A not developed; metapleuron and propodeum delimited with carina ..... ***Falsiformica cretacea* Rasnitsyn, 1975**

– Pedicel longer than 1st flagellomere (Engel 2022, fig. 2); fore wing with 2-A developed; metapleuron-propodeal boundary obliterated ..... ***Neophenax orcus* Engel, 2022**

4 2Rs distal of r-rs several times as long as r-rs; metabasitarsus longer than tarsomeres 2–4 combined **5**

– 2Rs distal of r-rs at most about as long as r-rs (Fig. 6E); metabasitarsus not longer than tarsomeres 2–4 combined (Fig. 5B) **8**

5 Cu well pigmented (Fig. 8C); 1st metasomal segment with long narrow part before node, making up more than one-third of its length ..... ***Siccibythus musculosus* Cockx & McKellar, 2016**

– Cu scarcely or not at all pigmented (Fig.1C); 1st metasomal segment with short part before node, making up less than one-third of its length (Fig. 1A) **6**

6 Scape at least 0.3 times as long as total length of flagellum (Rasnitsyn et al. 2020, fig. 7C) ..... ***Siccibythus paulus* Rasnitsyn, Zhang, Müller & Zhang, 2020**

– Scape distinctly shorter, less than 0.3 times total length of flagellum (Rasnitsyn et al. 2020, fig. 5B) 7

7 Anterior outline of 1st metasomal tergum straight; propodeum outline smoothly curved (Rasnitsyn et al. 2020, fig. 5) ..... ***Siccibythus ohmkuhnlei* Rasnitsyn, Zhang, Müller & Zhang, 2020**

– Anterior outline of 1st metasomal tergum somewhat angular, propodeum outline angular (Fig. 1A) ..... ***Siccibythus robustus* sp. nov.**

8 Fore wing length 3.5 mm; Rs+M and Cu distinctly pigmented (Rasnitsyn et al. 2020, fig. 4C); 4th tarsomere very short dorsally (with 5th tarsomere attached near 4th tarsomere's base) and much longer ventrally, its dorsal length 0.3 times length of 5th tarsomere ..... ***Siccibythus martynovae* Rasnitsyn, Zhang, Müller & Zhang, 2020**

– Fore wing length 2.5 mm or less; Rs+M and Cu not pigmented (Fig. 6E); 4th tarsomere elongate, deeply excised dorsally, its dorsal length 0.8 times length of 5th tarsomere **9**

9 Fore wing with 2-A partially pigmented; calcar's length approximately 0.3 times that of fore femur; fore wing length 1.75 mm..... ..... ***Siccibythus pallidus* Rasnitsyn, Zhang, Müller & Zhang, 2020**

– Fore wing with 2-A not pigmented (except for very base); calcar's length less than 0.2 times that of fore femur **10**

10 Pronotum with dorsal surface distinctly elongate; propodeal horns short, barely protruding; female flagellum not widened (Rasnitsyn et al. 2020, fig. 2)..... ***Siccibythus oculatus* Rasnitsyn, Zhang, Müller & Zhang, 2020**

– Pronotum with dorsal surface subquadrate; propodeal horns long, clearly protruding (Fig. 6C); female flagellum widened preapically (Fig. 6A) .... ***Siccibythus aristovi* sp. nov.**

Discussion

We assign the two species described here to †Falsiformicidae because of the sexual dimorphism in the number of antennomeres (females 12/males 13); notauli and parapsides present; fore wing venation reduced; hind wing with no closed cells and first metasomal tergum node-like. The new specimens exhibit consistent features, indicating that they belong to the same genus. They are distinguished from †*Falsiformica* and †*Neophenax* in having the fore wing 1m-cu not entirely tubular and dorsal surface of pronotum elongate or, rarely, subquadrate (Rasnitsyn 1975; Engel 2022); they are fully winged and differ from the brachypterous male †*Falsiformix*, whose fore wings are the approximately the same length as the mesosoma (Zhang et al. 2024). The flightlessness was discussed in Zhang et al. 2024. The new specimens are diagnostic features of †*Siccibythus*.

Engel (2022) considered †Falsiformicidae similar to Chrysidoidea in having lost the metespisternal-propodeal suture, reduced fore wing venation, three labial palpomeres, a constricted metapostnotum, and a usually broad propodeum with areolate sculpture. However, the metepisternal-propodeal boundary is well traceable in some †Falsiformicidae (Fig. 2B; Rasnitsyn 1975, fig. 126a). Reduced fore wing venation is likely homoplastic, yet the venation of Chrysidoidea other than Plumariidae and †Plumalexiidae is really characteristic, with tubular veins lost distally of 1m-cu, r-m (with at most a single vein distal to this) and 2cu-a, except for developed pterostigma, 2r-rs and RS distad of 2r-rs. However, similar venation is known in some non-chrysidoid Aculeata such as Sierolomorphidae and †Holopsenellidae, whose position within non-chrysidoid aculeates is well established (Lepeco and Melo 2022). A broad propodeum with areolate sculpture is known among non-chrysidoid aculeates as well, for instance, in †*Cretofedtschenkia santanensis* Ostin, 2007 (fig. 11.72b, in Martill et al. 2007); and in *Tiphia* spp. (Tiphiidae, cf. Goulet and Huber 1993, p. 162, figs 47–48). Four labial palpomeres are known both in †Falsiformicidae (Fig. 6B herein) and in Chrysidoidea (Lepeco and Melo 2024, Appendix 1, Character 8). The metapostnotum forms a rather wide, cross-ridged trough in †Falsiformicidae (Figs 2A, 4A) similar to that in *Sierolomorpha* (cf. Lelej and Mokrousov 2015: fig. 5).

Table 2. Comparison of characteristics between †Falsiformicidae, Chrysidoidea, and non-chrysidoid aculeates.

†Falsiformicidae	Chrysidoidea	non-chrysidoid aculeates
Metepisternal-propodeal boundary clearly distinguishable	-	+
Simplified forewing venation	+	+
Constricted metapostnotum	+	-
Usual broad propodeum with areolate sculpture	+	-
Broad propodeum with areolate sculpture	-	+
Metapostnotum forms a relatively wide trough with cross-ridged sculpturing	-	+
Sexual dimorphism in antennomere count	-	+

At the same time, †Falsiformicidae differ from Chrysidoidea and are similar to non-chrysidoid aculeates in the sexual dimorphism in the number of antennomeres (12 in females and 13 in males) and the 7th metasomal tergum internal in repose (Rasnitsyn et al. 2020). Specifically, sexual dimorphism in antennomere number in non-chrysidoid aculeates is highly stable, whereas it is not characteristic of Chrysidoidea (Sclerogibbidae is an exception, but they have 14–39 antennomeres, and the dimorphic figures of their antennomere numbers are not stabilized; Perkovsky et al. 2020, table 2). An internalized female tergum VII does occur within Chrysididae, where it results specifically from the transformation of several entire apical metasomal segments into an ovipositing device to regain the function lost due to the transformation of the ovipositor into a sting. In contrast, internalization of the seventh tergum in non-chrysidoid aculeates occurred due to a different process of ventilation of the metasoma via the last pair of enlarged spiracles hidden under the sixth metasomal tergum (Oeser 1961; Kimsey and Bohart 1991).

Based on the above analysis, the taxonomic position of †Falsiformicidae cannot yet be determined with certainty, comparison of characteristics between †Falsiformicidae, Chrysidoidea, and non-chrysidoid aculeates are listed in Table 2. More specimens and a comprehensive phylogenetic analysis would help to resolve this issue.

Acknowledgements

We thank the editorial board of Journal of Hymenoptera Research, and in particular Dr. Michael Ohl and Dr. Brendon Boudinot. We thank two reviewers for their valuable comments on this manuscript. We thank to Ms Weiwei Wang and Ms Yongfei Wang for their assistance with the measurement data. T.P.G was supported by the National Natural Science Foundation of China (Nos 32470468, 32020103006). A.P.R. was partially supported by the Presidium of the Russian Academy of Sciences Program "Origin of the Biosphere and Evolution of Geobiological Systems." E.E.P. was partially supported by the Scholars at Risk Ukraine (SARU) program, jointly funded by the Villum Foundation, the Carlsberg Foundation, and the Novo Nordisk Foundation.

References

Boudinot BE, Fisher BL (2013) A taxonomic revision of the *Meranoplus* F. Smith of Madagascar (Hymenoptera: Formicidae: Myrmicinae) with keys to species and diagnosis of the males. Zootaxa 3635: 301–339. https://doi.org/10.11646/zootaxa.3635.4.1

Cockx PFD, McKellar RC (2016) First record of the family Scolebythidae (Hymenoptera) in mid-Cretaceous amber from Myanmar. Cretaceous Research 67: 133–139. https://doi.org/10.1016/j.cretres.2016.06.015

Cruickshank RD, Ko K (2003) Geology of an amber locality in the Hukawng Valley, Northern Myanmar. Journal of Asian Earth Sciences 21: 441–455. https://doi.org/10.1016/S1367-9120(02)00044-5

Dlussky GM (1996) Ants (Hymenoptera: Formicidae) from Burmese amber. Paleontological Journal 30 (4): 449–454.

Engel MS (2022) The first New World Falsiformicidae (Hymenoptera): a new genus in Upper Cretaceous amber from New Jersey. Entomologist's Monthly Magazine 158: 157–168. https://doi:10.31184/M00138908.1583.4100

Goulet H, Huber JT (1993) Hymenoptera of the world: An identification guide to families. Canadian Communication Group (Canadian): 1–668.

Heine C, Müller RD, Gaina C (2004) Reconstructing the lost eastern Tethys ocean basin: convergence history of the SE Asian margin and marine gateways. Geophysical Monograph Series 149: 1–18. https://doi.org/10.1029/149GM03

International Commission on Zoological Nomenclature (1999) International Code of Zoological Nomenclature (4th ed.). London: International Trust for Zoological Nomenclature.

Kimsey LS, Bohart RM (1991 [1990]) The Chrysidid Wasps of the World. Oxford Science Publications, 652 pp. https://doi.org/10.1093/oso/9780198540106.001.0001

Lelej AS, Mokrousov MV (2015) *Sierolomorpha sogdiana* spec. nov. from Central Asia, and a World catalogue of Sierolomorphidae (Hymenoptera). Zootaxa 4018 (4): 593–599. http://dx.doi.org/10.11646/zootaxa.4018.4.8

Lepeco A, Melo GAR (2022) The wasp genus †*Holopsenella* in mid-Cretaceous Burmese amber (Hymenoptera: †Holopsenellidae stat. nov.). Cretaceous Research 131: 105089. https://doi.org/10.1016/j.cretres.2021.105089

Lepeco A, Melo GAR (2024) Revisiting the phylogeny of the scolebythid wasps (Hymenoptera: Aculeata) through Bayesian model evaluation and parsimony, with description of a new fossil family of Chrysidoidea. Zoological Journal of the Linnean Society 201: 57–85. https://doi.org/10.1093/zoolinnean/zlad113

Lucena DA, Melo GAR (2018) Chrysidid wasps (Hymenoptera: Chrysididae) from Cretaceous Burmese amber: Phylogenetic affinities and classification. Cretaceous Research 89: 279–291. https://doi.org/10.1016/j.cretres.2018.03.018

Martill DM, Bechly G, Loveridge RF (2007) The Crato Fossil Beds of Brazil. Window into an Ancient World. Camdridge, etc., Cambridge University Press, xvi + 625 pp. https://doi.org/10.1017/CBO9780511535512

Oeser R (1961) Vergleichend-morphologische Untersuchungen über den Ovipositor der Hymenopteren. Mitteilungen aus dem Zoologischen Museum Berlin 37: 3–119. https://doi.org/10.1002/mmnz.19610370102

Perkovsky EE, Martynova KV, Mita T, Olmi M, Zheng Y, Müller P, Zhang Q, Gantier F, Perrichot V (2020) A golden age for ectoparasitoids of Embiodea: Cretaceous Sclerogibbidae (Hymenoptera, Chrysidoidea) from Kachin (Myanmar), Charentes (France) and Choshi (Japan) ambers. Gondwana Research 87: 1–22. https://doi.org/10.1016/j.gr.2020.06.004

Perrichot V, Engel MS, Nel A, Ortega-Blanco J, Delclòs X, Soriano C, Lohrmann V, Tafforeau P (2014) "False ants" from the Cretaceous (Hymenoptera: Chrysidoidea: †Falsiformicidae). Mitteilungen des Entomologischen Vereins Stuttgart 49: 26.

Poinar GJ (2018) Burmese amber: evidence of Gondwanan origin and Cretaceous dispersion. Historical Biology 31: 1304–1309. https://doi.org/10.1080/08912963.2018.1446531

Rasnitsyn AP (1975) Hymenoptera Apocrita of Mesozoic. Transaction of the Paleontological Institute, Academy of Sciences of the USSR 147: 1–134.

Rasnitsyn AP, Zhang Q, Müller P, Zhang HC (2020) On the identity and limits of Falsiformicidae (Insecta: Hymenoptera, Vespoidea s.l.). Palaeoentomology 3: 582–596. https://doi.org/10.11646/palaeoentomology.3.6.10

Ross AJ (2024) Complete checklist of Burmese (Myanmar) amber taxa 2023. Mesozoic 1: 21–57. https://doi.org/10.11646/mesozoic.1.1.4

Schödl S (2007) Revision of Australian *Meranoplus*: the *Meranoplus diversus* group. In: Snelling R, Fisher B, Ward P (Eds) Advances in ant systematics: Homage to E.O. Wilson. The American Entomological Institute (Florida): 370–424.

Seton M, Müller RD, Zahirovic S, Gaina C, Torsvik T, Shepard G, Talsma, A, Gurnis M, Turner M, Maus S, Chandler M (2012) Global continental and ocean basin reconstructions since 200 Ma. Earth-Science Review 113: 212–270. https://doi.org/10.1016/j.earscirev.2012.03.002

Sevastjanova I, Hall R, Rittner M, Lay Paw SMT, Naing TY, Alderton DH, Comfort G (2016) Myanmar and Asia united, Australia left behind long ago. Gondwana Research 32: 24–40. https://doi.org/10.1016/j.gr.2015.02.001

Shi G, Grimaldi DA, Harlow GE, Wang J, Wang J, Yang M, Lei W, Li Q, Li X (2012) Age constraint on Burmese amber based on U–Pb dating of zircons. Cretaceous Research 37: 155–163. https://doi.org/10.1016/j.cretres.2012.03.014

Szwedo J, Wang B, Soszynska-Maj A, Azar D, Ross A, 2020. International Palaeoentomological Society Statement. Palaeoentomology 3: 221–222. https://doi.org/10.11646/palaeoentomology.3.3.1

Wang Z, Vilhelmsen L, Rasnitsyn AP, Viertler A, Shih CK, Wen SS, Yang HR, Wu Q, Zhang YJ, Ren D, Gao TP (2024) Specialized ovipositor sensilla of Cretaceous wasp (Insecta: Hymenoptera) possibly reveal a unique way of host detection. Cladistics 40: 526–537. https://doi.org/10.1111/cla.12579

Westerweel J, Roperch P, Licht A, Dupont-Nivet G, Win Z, Poblete F, Ruffet G, Swe HH, Thi MK, Aung DW (2019) Burma Terrane part of the Trans-Tethyan arc during collision with India according to palaeomagnetic data. Nature Geoscience 12: 863–868. https://doi.org/10.1038/s41561-019-0443-2

Wu Q, Radchenko A, Engel MS, Li XQ, Yang HR, Li XR, Shih CK, Ren D, Gao TP (2024) Cretaceous crown male ant reveals the rise of modern lineages. Zoological Research 45(5): 983–989. https://doi.org/10.24272/j.issn.2095-8137.2023.390

Yang HR, Engel MS, Shih CK, Song F, Zhao YS, Ren D, Gao TP (2023) Independent wing reductions and losses among stick and leaf insects (Phasmatodea), supported by new Cretaceous fossils in amber. BMC Biology 21: 210. https://doi.org/10.1186/s12915-023-01720-0

Zhang Q, Rasnitsyn AP, Wang B, Zhang HC (2018) Hymenoptera (wasps, bees and ants) in mid-Cretaceous Burmese amber: A review of the fauna. Proceedings of the Geologists Association 129: 736–747. https://doi.org/10.1016/j.pgeola.2018.06.004

Zhang Q, Jia N, Li YZ, Wang JX, Rasnitsyn AP (2024) New genus of falsiformicid wasps (Hymenoptera, Vespoidea: Falsiformicidae) with brachypterous male from middle Cretaceous Kachin amber in Myanmar. Cretaceous Research. https://doi.org/10.1016/j.cretres.2024.106057

Supplementary material 1

The measurements of the specimen (mm)

Authors: Zhen Wang, Alexandr P. Rasnitsyn, Evgeny E. Perkovsky, Lars Vilhelmsen, Taiping Gao

Data type: xlsx

Copyright notice: This dataset is made available under the Open Database License (http://opendatacommons.org/licenses/odbl/1.0/). The Open Database License (ODbL) is a license agreement intended to allow users to freely share, modify, and use this Dataset while maintaining this same freedom for others, provided that the original source and author(s) are credited.

Link: https://doi.org/10.3897/jhr.98.136200.suppl1

Supplementary material 2

Measurements and standard deviation analysis of CNU-HYM-MA2016212 (mm)

Authors: Zhen Wang, Alexandr P. Rasnitsyn, Evgeny E. Perkovsky, Lars Vilhelmsen, Taiping Gao

Data type: xlsx

Copyright notice: This dataset is made available under the Open Database License (http://opendatacommons.org/licenses/odbl/1.0/). The Open Database License (ODbL) is a license agreement intended to allow users to freely share, modify, and use this Dataset while maintaining this same freedom for others, provided that the original source and author(s) are credited.

Link: https://doi.org/10.3897/jhr.98.136200.suppl2